

# Spatially Resolved Streaming Potentials of Human Intervertebral Disk Motion Segments Under Dynamic Axial Compression

**James C. Iatridis<sup>1</sup>**

School of Engineering,  
Department of Orthopaedics and Rehabilitation,  
University of Vermont,  
33 Colchester Avenue,  
Burlington, VT 05405  
e-mail: james.iatridis@uvm.edu

**Masaru Furukawa**

**Ian A. F. Stokes**

**Mack G. Gardner-Morse**

Department of Orthopaedics and Rehabilitation,  
University of Vermont,  
Burlington, VT 05405

**Jeffrey P. Laible**

School of Engineering,  
University of Vermont,  
Burlington, VT 05405

*Intervertebral disk degeneration results in alterations in the mechanical, chemical, and electrical properties of the disk tissue. The purpose of this study is to record spatially resolved streaming potential measurements across intervertebral disks exposed to cyclic compressive loading. We hypothesize that the streaming potential profile across the disk will vary with radial position and frequency and is proportional to applied load amplitude, according to the presumed fluid-solid relative velocity and measured glycosaminoglycan content. Needle electrodes were fabricated using a linear array of Ag/AgCl micro-electrodes and inserted into human motion segments in the midline from anterior to posterior. They were connected to an amplifier to measure electrode potentials relative to the saline bath ground. Motion segments were loaded in axial compression under a preload of 500 N, sinusoidal amplitudes of  $\pm 200$  N and  $\pm 400$  N, and frequencies of 0.01 Hz, 0.1 Hz, and 1 Hz. Streaming potential data were normalized by applied force amplitude, and also compared with paired experimental measurements of glycosaminoglycans in each disk. Normalized streaming potentials varied significantly with sagittal position and there was a significant location difference at the different frequencies. Normalized streaming potential was largest in the central nucleus region at frequencies of 0.1 Hz and 1.0 Hz with values of approximately  $3.5 \mu\text{V}/\text{N}$ . Under 0.01 Hz loading, normalized streaming potential was largest in the outer annulus regions with a maximum value of  $3.0 \mu\text{V}/\text{N}$ . Correlations between streaming potential and glycosaminoglycan content were significant, with  $R^2$  ranging from 0.5 to 0.8. Phasic relationships between applied force and electrical potential did not differ significantly by disk region or frequency, although the largest phase angles were observed at the outermost electrodes. Normalized streaming potentials were associated with glycosaminoglycan content, fluid, and ion transport. Results suggested that at higher frequencies the transport of water and ions in the central nucleus region may be larger, while at lower frequencies there is enhanced transport near the periphery of the annulus. This study provides data that will be helpful to validate multiphasic models of the disk. [DOI: 10.1115/1.3005164]*

*Keywords: intervertebral disk, disk degeneration, streaming potential, fixed charge density, fluid flow, dynamic compression*

## Introduction

Intervertebral disks (IVDs) function mechanically to support high compressive loads and shear deformations while permitting rotational flexibility. The IVD mechanical behaviors are related to the highly organized annular structure and gel-like nucleus, which provides a strong regional variation in tissue material properties and composition [1]. IVD degeneration results in substantial changes in the material and structural properties, which are associated with loss of spinal stability and pain [2]. IVD cells are sensitive to loading, which may be associated with mechanotransduction as well as alterations in load-induced solute transport [3]. In cartilaginous tissues, electrical potentials are passively elicited by fluid flow resulting from mechanical compression of charged porous tissues and are called streaming potentials. Streaming po-

tentials have been suggested to be useful for evaluating cartilage integrity and may stimulate chondrocyte biosynthesis [4–8]. In cartilage these signals vary with region, position, frequency, and ionic strength [9].

Streaming potentials are also associated with fluid flow through the charged porous solid matrix of the intervertebral disk. An explicit relationship of streaming potentials as a function of applied pressure in a 1D permeation experiment at steady state was described by

$$\kappa \Delta \Phi = -c^F F_c k \Delta p = -c^F F_c \dot{w} \quad (1)$$

where  $\kappa$  is electrical conductivity,  $\Delta \Phi$  is streaming potential,  $c^F$  is fixed charge density,  $F_c$  is the Faraday constant,  $k$  is permeability,  $\Delta p$  is applied pressure, and  $\dot{w}$  is relative fluid velocity [10]. In three dimensions, a complex functional relationship is necessary to express the dependence of streaming potential on fixed charge density, electrical conductivity, ion concentrations, and parameters that influence fluid velocity including porosity, permeability, stiffness, and boundary conditions [8,11–13]. However, based on symmetry of the disk across the midsagittal and midtransverse planes,

<sup>1</sup>Corresponding author.

Contributed by the Bioengineering Division of ASME for publication in the JOURNAL OF BIOMECHANICAL ENGINEERING. Manuscript received October 5, 2007; final manuscript received August 20, 2008; published online January 6, 2009. Review conducted by Jacques M. Huyghe.

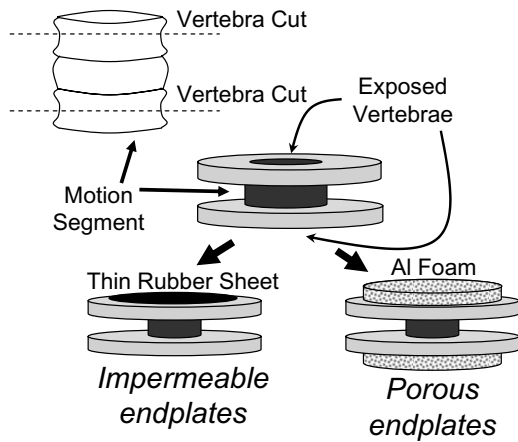


**Fig. 1 Schematic representation of specimen preparation with two different boundary conditions in order to adjust vertebral endplate permeability**

alterations in streaming potential under pure compressive loading may be assumed to vary along a 1D line in the sagittal plane across the anterior-posterior midline, and may be adequately measured with a linear electrode array.

Streaming potential may be a sensitive indicator of intervertebral disk degeneration since permeability, fixed charge density, and disk stiffness are all altered with disk degeneration in a regionally specific manner [1,10,12,14–16]. Measurements of streaming potential in a region specific manner of an intact disk have not been reported and would be necessary to assess whether this parameter may be used to provide information on the physics of the disk under loading and how it changes with degeneration.

We hypothesized that streaming potentials in the intervertebral disk in situ will be affected by disk region and frequency of loading because of the strong regional variations in proteoglycan content, permeability, and stiffness, and because loading frequency is expected to affect fluid flow in regionally specific manners. The objectives of this study were to fabricate and implant a needle electrode for measurement of spatially resolved streaming potentials in intact human intervertebral disks and to evaluate how streaming potentials are affected by disk region, dynamic loading, magnitude, and frequency. Experimental measurements were made on cadaveric human IVDs with a relatively narrow band of degenerative grade ranging from mild to moderate.

## Methods

Human motion segments ( $n=9$ , age=53–56 years, levels=L2-3 and L3-4) were prepared by cutting through the midtransverse plane of two adjacent vertebrae, removing posterior elements and transverse processes, and embedding in polymethyl methacrylate (Fig. 1) with the discs and cut surfaces of the vertebrae left exposed.

Needle electrodes were fabricated using a linear array of Ag/AgCl micro-electrodes fabricated using eight H-polynylon coated silver wires (142  $\mu\text{m}$  diameter, California Fine Wire Company, Grover Beach, CA). Wires were wound together and cut at intervals such that the exposed tips were spaced evenly 4 mm apart to form a bundle (Fig. 2). The exposed (uninsulated) wire ends served as micro-electrodes that were chloridized as previously described [17]. Briefly, electrodes were chloridized by electrolysis using a constant 1.5 V dc power supply in a 0.1M HCl bath for 3 min. The electrical resistance between two Ag–AgCl electrodes was measured in saline using a 1 Hz, 500 mV input sine wave and found to be 6.3 k $\Omega$ , much lower than the 100 M $\Omega$  input impedance of the amplifier. The electrode bundle was inserted from anterior to posterior through the midtransverse plane of each disk by threading the micro-electrodes through a 60 mm

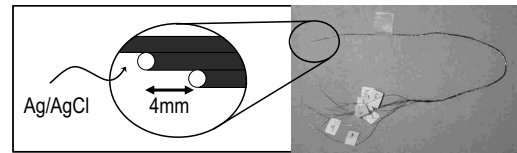


**Fig. 2 Construction detail of the linear array of eight Ag/AgCl micro-electrodes**

long, 18 gauge needle inserted in the disk. The needle was then removed and the electrodes remained in the disk for mechanical testing (Fig. 3). The first electrode in the array was placed in the posterior annulus, and the next to the last one was near the anterior margin of the disk. The last wire was grounded to a large Ag/AgCl electrode placed in the saline bath (Fig. 3). The wires were connected to an eight-channel variable gain dc amplifier (Model 208B, Trig-Tek, Anaheim, CA) in order to measure differential potentials between electrodes relative to the saline ground, and interfaced with a digital data acquisition system. Each motion segment was placed in a saline bath on a testing machine (MTS Systems, Minneapolis, MN) and loaded axially. The specimens were first equilibrated at an initial preloading condition of 500 N for 2 h followed by test loads of six cycles of a sinusoidal wave at two amplitudes ( $\pm 200$  N and  $\pm 400$  N, which are in the low physiological range) and three frequencies (0.01 Hz, 0.1 Hz, and 1 Hz).

In a preliminary experiment, specimens were loaded with both porous and impermeable boundary conditions using either a rigid aluminum filter to allow fluid exchange or a thin rubber sheet that prevented fluid flow through the exposed surface (Fig. 1). No significant effects ( $p=0.22$ ) of endplate permeability boundary condition (porous platen versus rubber sheet) were detected with mean  $\pm$  SEM (standard error of the mean) slopes of the displacement-force curves at 1 Hz of  $0.54 \pm 0.02 \mu\text{m}/\text{N}$  and  $0.50 \pm 0.02 \mu\text{m}/\text{N}$  for the porous and impermeable cases, respectively. It was assumed that there would be no boundary condition effects on measured streaming potential but this was not verified. All nine specimens were therefore tested with only the impermeable endplate condition. Force, displacement, and electrical potential data from each electrode (Fig. 4) were recorded.

The streaming potential signals were analyzed with custom software written in MATLAB (Mathworks, Natick, MA). Electrical data were first low pass filtered ( $-3$  db at 10 Hz) to remove high frequency noise and detrended to remove dc offset caused by electrode imbalances or viscoelastic creep. Fast Fourier transformation (FFT) was then used to extract the amplitude and phase angle between the recorded potential and the applied load or displacement at the fundamental frequency. Streaming potentials were normalized to ease comparisons within this study and across other studies. The correlation of electrical potential with applied load was greater than that with disk compression displacement (mean  $R^2=0.74$  versus 0.72,  $p < 0.0001$ , paired t-test), and therefore streaming potentials were expressed as the gradient of the potential-force relationship (mV/N).

Once testing was completed, disks were graded, and evaluated for glycosaminoglycan content, as previously described [15]. Degenerative grade of each disk was recorded according to Thompson's scale modified for the use of transverse sections [18]. All glycosaminoglycan (GAG) content measurements were performed in duplicate, and GAG was presented as a function of sagittal dimensions [15].

Normalized streaming potentials and phase angle were analyzed with two-factor analysis of variance (ANOVA) (factors: electrode radial position and frequency). The effects of endplate permeability conditions on disk stiffness were evaluated with paired t-tests. A linear regression analysis was performed to evaluate the correlation between average GAG content with average values for normalized streaming potential at each frequency of

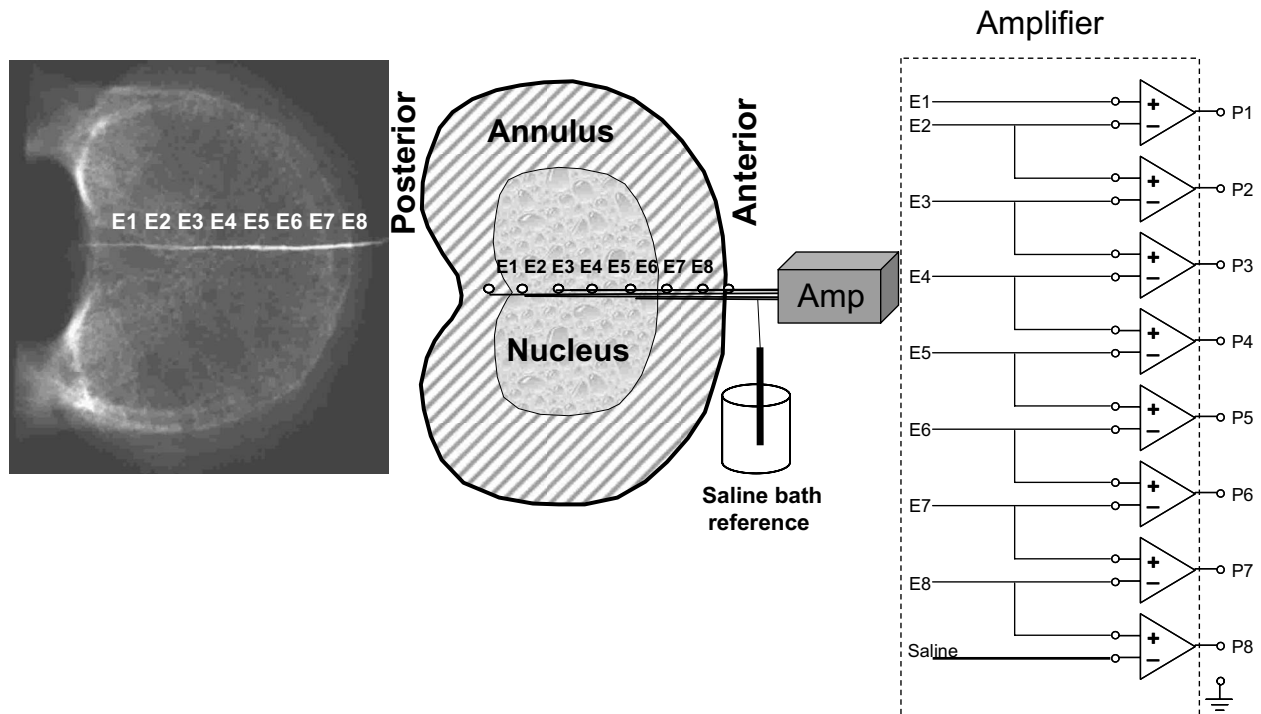


**Fig. 3** Electrodes were inserted from anterior to posterior in the disk using 18 gauge needles and connected to amplifiers

loading. All analyses were performed using STATVIEW software (SAS Institute, Cary, NC).

### Results

Streaming potentials normalized by applied force were significantly different by radial position ( $p < 0.0001$ ) and there was a significant interaction between frequency and radial position ( $p$

$= 0.01$ ), but there was only a nonsignificant trend of streaming potential with frequency ( $p = 0.1$ ) having lesser amplitude in the central portion of the disk (Fig. 5). The correlations between electrical potential (non-normalized) and load amplitude were strong with mean  $\pm$  SD value of  $R^2 = 0.74 \pm 0.35$ , although the vast majority of correlations were very high with median value of 0.95. This correlation was significantly affected by radial position ( $p$

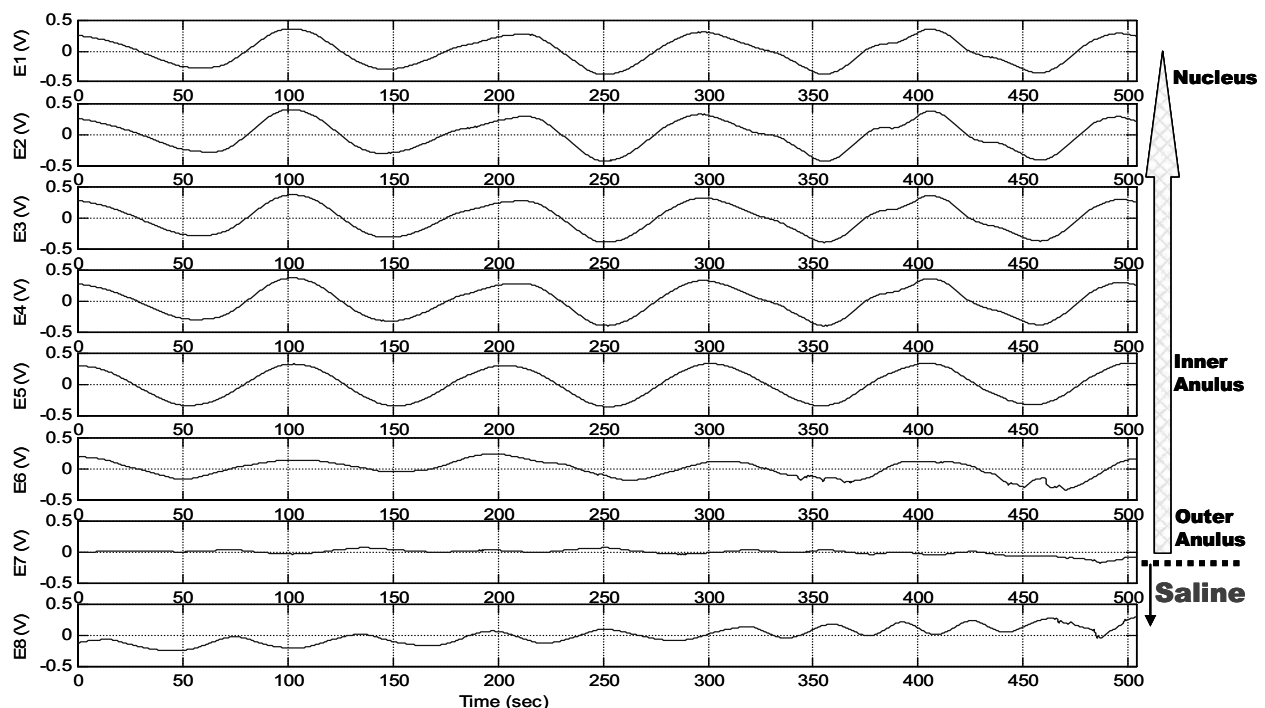


**Fig. 4** Sample data of amplified electrode potentials relative to bath potential

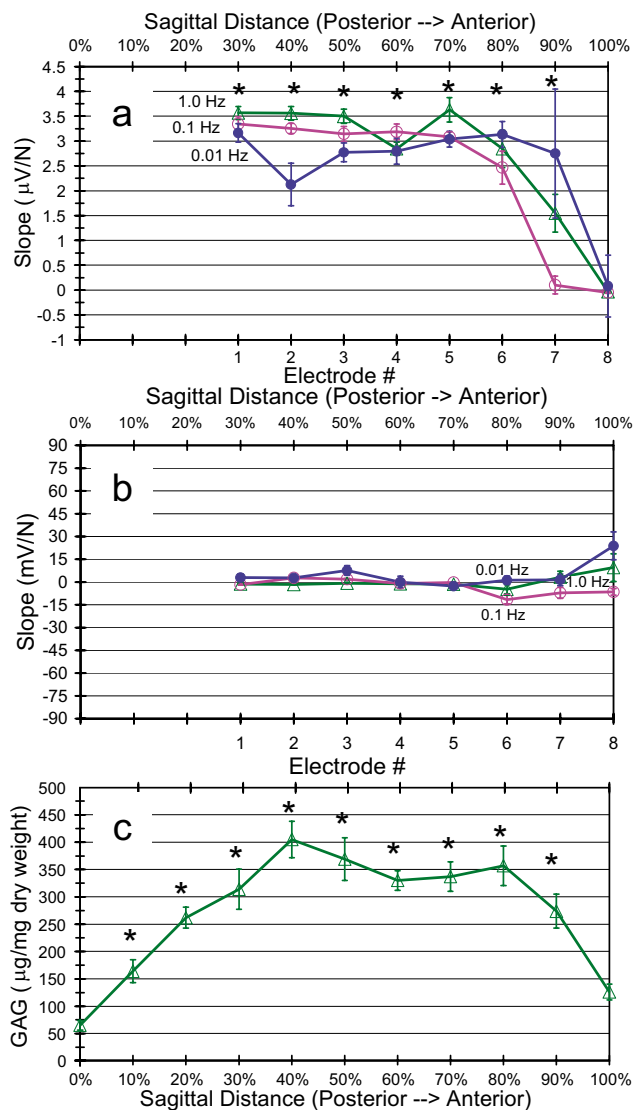


**Fig. 5 Mean±SEM ( $n=9$ ) for (a) streaming potential normalized by applied force amplitude, (b) phase angle between streaming potential and applied force as a function of electrode position with relative sagittal position on the upper x-axis. (c) GAG measurements with relative sagittal position. For streaming potential data, \* indicates significant ( $p<0.05$ ) difference from electrode 8 for all frequencies; although at 0.1 Hz electrode seven streaming potentials are not significantly different from electrode 8. For GAG measurements, \* indicates significant difference from value at 100%.**

$<0.0001$ ) and by frequency ( $p<0.0001$ ), with no significant interaction ( $p=0.24$ ) with the lowest values for the correlation occurring in electrodes at the outer annulus and at the lowest frequencies. The correlations had mean values of  $R^2>0.8$  (median value  $>0.95$ ) for electrodes 1–6 validating the linearity assumption used in the analysis of data, although the value of  $R^2<0.5$  (median value  $<0.4$ ) for electrodes 7 and 8 suggested more non-linear responses at the disk periphery. Normalized streaming potentials did not differ with load amplitude ( $p=0.50$  for streaming potential;  $p=0.97$  for phase angle).

The phase angle (representing a lag between the measured voltage and the force applied) was small (mean±SEM =  $0.5\pm 1.32$  deg), and was not significantly different from zero ( $p=0.71$ , t-test). The phase angle was independent of frequency

( $p=0.9$ ) and radial position ( $p=0.12$ ), with no significant interaction between frequency and radial position ( $p=0.9$ ).

All intervertebral disks were rated as either Thompson Grade 2 or 3 (two Grade 2 disks; seven Grade 3 disks) based on gross morphology, indicating mild to moderate signs of degeneration. GAG results indicated that there were significant effects of sagittal position with values ranging from  $\sim 40$   $\mu\text{g}/\text{mg}$  to  $600$   $\mu\text{g}/\text{mg}$  dry tissue (Fig. 5(c)). The highest values were in the nucleus and the lowest were in the outer annulus. There was also evidence of a midnuclear cleft with lower GAG values. Significant but moderate correlations were observed between regional GAG content values and normalized streaming potential values measured at the locations of the electrodes in the middle sagittal plane with  $p<0.05$  and adjusted  $R^2=0.52, 0.61, 0.80$  for frequencies of 0.01 Hz, 0.1 Hz, and 1 Hz, respectively.

## Discussion

This study developed and implemented a needle electrode system capable of measuring electrical streaming potentials in the human intervertebral disk under load. Needles were implanted from anterior to posterior where gradients in relative fluid velocity and concentrations were expected to be the largest based on symmetries along the midsagittal and midtransverse planes. We hypothesized that streaming potentials in the intervertebral disk would be affected by disk region and frequency of loading because of the strong regional variations in proteoglycan content, permeability, and stiffness, and because loading frequency is expected to affect fluid flow in regionally specific manners. Results indicated that the amplitudes of normalized streaming potentials were significantly affected by electrode number (i.e., radial position). This was expected because of the known radial variation in fixed charge density, stiffness, permeability, and fluid velocity. The interactions between frequency and radial position for the streaming potential response suggested frequency dependent variations in the localized values for these parameters that may suggest localized alterations in water or ion transport that change with loading frequency.

Streaming potential magnitudes in tissues are known to be associated with the fixed charge density, hydraulic permeability, electrical conductivity of the tissue, and applied pressure [10]. In cartilage tissues, streaming potential maps are sensitive to amplitude, frequency, and ionic strength of the solution around the tissue [9]. When considering the intact disk structure, the streaming potential also depends on disk tissue stiffness, hydraulic permeability, and intradiscal pressure. These are affected by loading magnitude and frequency in a localized manner. Alterations in the relative values of these parameters, as well as the extracellular water exchange [19], can impact these results strongly. This electric potential distribution reported here is similar to those reported in the multiphase finite element models of Ferguson et al. [20] and Yao and Gu [13], which demonstrated that electrical potentials were affected by changes in water content, fixed charge density, and modulus [13,20]. Differences between model and experimental results may be explained by idealized assumptions in the models as well as experimental variations from human specimens. The magnitudes are similar to, although somewhat larger than those presented in the one-dimensional experimental study by Gu et al. [10], which may be explained by differences in the load magnitudes and configurations with the current 3D experimental study.

By comparing similarities and differences between the radial variation of normalized streaming potential with variation of tissue fixed charge density (or GAG content as evaluated in this study), we can make some important observations and inferences associated with physics of disk behavior under loading. Firstly, the overall trend in normalized streaming potential follows the overall pattern of GAG content with significant and reasonably strong correlations (i.e., adjusted  $R^2$  values ranged between 0.52 and 0.8, depending on frequency). The correlation with fixed

charge was expected, but other factors were also at play in determining streaming potential, and water or positive ion transport are the strongest contributors. Secondly, in the central nucleus pulposus region, the shape of the normalized streaming potential is most similar to the GAG distribution at 0.01 Hz, with a notable dip in the central nucleus. This intranuclear cleft has previously been reported using magnetic resonance imaging (MRI), GAG, and radioactive tracers [15,21–23]. This suggests that loading at 0.1 Hz and 1 Hz results in more fluid or ion transport in the central nucleus, consistent with high levels of pressurization of the central nucleus under relatively high frequency loading. Thirdly, there is a rapid drop in the values of normalized streaming potential in the outer annulus and a more gradual drop in values of GAG, suggesting a role of fluid flow or ion transport in the outer annulus region where the fluid velocities are highest. It is also interesting that the largest values of normalized streaming potential in the outer annulus fibrosus occurred at 0.01 Hz loading and were lower for 0.1 Hz and 1 Hz, suggesting that in the outer annulus regions, the slower frequencies resulted in greater fluid transport. This finding is consistent with the findings of Masuoka et al. [24] that viscoelastic behaviors in the intervertebral disk under compression are associated with an initial disk bulge at short times (or rapid loading rates), and fluid loss and redistribution at longer times (or slower loading rates), which may affect localized transport patterns. Localized transport has also been demonstrated with enhanced transport of fluorophores, particularly through the endplate during diurnal cyclic loading in an organ culture system [25]. Modeling studies have also demonstrated that localized transport of varying molecular weight tracers is affected by loading conditions and duration of load [13,20]. Consequently, the normalized streaming potential results suggest that in the range of frequencies tested, fluid and ion transport may be larger in the central nucleus pulposus region at high frequencies and larger in the outer annulus fibrosus at lower frequencies. A larger array of electrodes and/or 3D computational model would be necessary to provide more information about water transport.

The permeability boundary condition at the midtransverse plane of the vertebral body had minimal effects on the load-displacement curve in preliminary experiments, suggesting that fluid flow between the disk and the vertebral body was relatively small under our testing conditions. A recent study indicated that boundary conditions along the vertebral body had a small effect on intervertebral disk recovery under loading [26]. However, it is known that removal of vertebral bodies can have a substantial effect on viscoelastic behaviors of the intervertebral disk [27]. Furthermore, blood clots in the capillary buds of cadaveric intervertebral disks can impede flow and diffusion, and have been demonstrated to result in cell death in a bovine organ culture model [28] while use of an anticoagulant permitted transport via the endplate [25]. Consequently, in order to evaluate accurately the effects of endplate permeability on viscoelastic and streaming potential responses, it is likely that the permeability of the vertebral endplate boundary must be free of blood clots prior to modification of the permeability of the loading platen.

In conclusion, this study provided streaming potential measurements of disk specimens with a relatively narrow band of degenerative grade (mild to moderate). Streaming potential measurements exhibited profiles that were similar to fixed charge density distributions with some small differences that may be associated with alterations in fluid transport at different frequencies of loading. Future experimental measurements will be necessary to evaluate the sensitivity of streaming potentials to degenerative grade and to explore more fully the 3D fluid transport patterns in the disk.

## Acknowledgment

This work is supported by Grant Nos. R01 AR 049370 and R01 AR 051146 from the National Institutes of Health. Disk speci-

mens were supplied by National Disease Research Interchange (NDRI).

## References

- [1] Stokes, I. A. F., and Iatridis, J. C., 2004, "Biomechanics of the spine," *Basic Orthopaedic Biomechanics and Mechano-Biology*, V. C. Mow and R. Huiskes, eds., Lippincott, Williams, & Wilkins, New York.
- [2] Adams, M. A., and Roughley, P. J., 2006, "What is Intervertebral Disc Degeneration, and What Causes It?," *Spine*, **31**(18), pp. 2151–2161.
- [3] Setton, L. A., and Chen, J., 2006, "Mechanobiology of the Intervertebral Disc and Relevance to Disc Degeneration," *J. Bone Jt. Surg., Am. Vol.*, Vol. **88**(2), pp. 52–57.
- [4] Binette, J. S., Garon, M., Savard, P., McKee, M. D., and Buschmann, M. D., 2004, "Tetrapolar Measurement of Electrical Conductivity and Thickness of Articular Cartilage," *ASME J. Biomech. Eng.*, **126**(4), pp. 475–484.
- [5] Chen, A. C., Nguyen, T. T., and Sah, R. L., 1997, "Streaming Potentials During the Confined Compression Creep Test of Normal and Proteoglycan-Depleted Cartilage," *Ann. Biomed. Eng.*, **25**(2), pp. 269–277.
- [6] Kim, Y. J., Bonassar, L. J., and Grodzinsky, A. J., 1995, "The Role of Cartilage Streaming Potential, Fluid Flow and Pressure in the Stimulation of Chondrocyte Biosynthesis During Dynamic Compression," *J. Biomech.*, **28**(9), pp. 1055–1066.
- [7] Sachs, J. R., and Grodzinsky, A. J., 1995, "Electromechanical Spectroscopy of Cartilage Using a Surface Probe With Applied Mechanical Displacement," *J. Biomech.*, **28**(8), pp. 963–976.
- [8] Sun, D. D., Guo, X. E., Likhithpanichkul, M., Lai, W. M., and Mow, V. C., 2004, "The Influence of the Fixed Negative Charges on Mechanical and Electrical Behaviors of Articular Cartilage Under Unconfined Compression," *ASME J. Biomech. Eng.*, **126**(1), pp. 6–16.
- [9] Garon, M., Legare, A., Guardo, R., Savard, P., and Buschmann, M. D., 2002, "Streaming Potentials Maps are Spatially Resolved Indicators of Amplitude, Frequency and Ionic Strength Dependent Responses of Articular Cartilage to Load," *J. Biomech.*, **35**(2), pp. 207–216.
- [10] Gu, W. Y., Mao, X. G., Rawlins, B. A., Iatridis, J. C., Foster, R. J., Sun, D. N., Weidenbaum, M., and Mow, V. C., 1999, "Streaming Potential of Human Lumbar Annulus Fibrosus is Anisotropic and Affected by Disc Degeneration," *J. Biomech.*, **32**(11), pp. 1177–1182.
- [11] Gu, W. Y., Lai, W. M., and Mow, V. C., 1993, "Transport of Fluid and Ions Through a Porous-Permeable Charged-Hydrated Tissue, and Streaming Potential Data on Normal Bovine Articular Cartilage," *J. Biomech.*, **26**(6), pp. 709–723.
- [12] Iatridis, J. C., Laible, J. P., and Krag, M. H., 2003, "Influence of Fixed Charge Density Magnitude and Distribution on the Intervertebral Disc: Applications of a Poroelectric and Chemical Electric (PEACE) Model," *ASME J. Biomech. Eng.*, **125**(1), pp. 12–24.
- [13] Yao, H., and Gu, W. Y., 2007, "Three-Dimensional Inhomogeneous Triphasic Finite-Element Analysis of Physical Signals and Solute Transport in Human Intervertebral Disc Under Axial Compression," *J. Biomech.*, **40**(9), pp. 2071–2077.
- [14] Gu, W. Y., Mao, X. G., Foster, R. J., Weidenbaum, M., Mow, V. C., and Rawlins, B. A., 1999, "The Anisotropic Hydraulic Permeability of Human Lumbar Annulus Fibrosus. Influence of Age, Degeneration, Direction, and Water Content," *Spine*, **24**(23), pp. 2449–2455.
- [15] Iatridis, J. C., MacLean, J. J., O'Brien, M., and Stokes, I. A., 2007, "Measurements of Proteoglycan and Water Content Distribution in Human Lumbar Intervertebral Discs," *Spine*, **32**(14), pp. 1493–1497.
- [16] Urban, J. P., and McMullin, J. F., 1988, "Swelling Pressure of the Lumbar Intervertebral Discs: Influence of Age, Spinal Level, Composition, and Degeneration," *Spine*, **13**(2), pp. 179–187.
- [17] Baker, L. E., and Geddes, L. A., 1969, *Principles of Applied Biomedical Instrumentation*, Wiley, New York.
- [18] Thompson, J. P., Pearce, R. H., Schechter, M. T., Adams, M. E., Tsang, I. K., and Bishop, P. B., 1990, "Preliminary Evaluation of a Scheme for Grading the Gross Morphology of the Human Intervertebral Disc," *Spine*, **15**(5), pp. 411–415.
- [19] Schroeder, Y., Sivan, S., Wilson, W., Merker, Y., Huyghe, J. M., Maroudas, A., and Baaijens, F. P., 2007, "Are Disc Pressure, Stress, and Osmolarity Affected by Intra- and Extracellular Fluid Exchange?," *J. Orthop. Res.*, **25**(10), pp. 1317–1324.
- [20] Ferguson, S. J., Ito, K., and Nolte, L. P., 2004, "Fluid Flow and Convective Transport of Solutes Within the Intervertebral Disc," *J. Biomech.*, **37**(2), pp. 213–221.
- [21] Houghton, V., 2006, "Imaging Intervertebral Disc Degeneration," *J. Bone Jt. Surg., Am. Vol.*, Vol. **88**(2), pp. 15–20.
- [22] Perry, J., Houghton, V., Anderson, P. A., Wu, Y., Fine, J., and Mistretta, C., 2006, "The Value of T2 Relaxation Times to Characterize Lumbar Intervertebral Discs: Preliminary Results," *AJNR Am. J. Neuroradiol.*, **27**(2), pp. 337–342.
- [23] Urban, J. P. G., and Maroudas, A., 1979, "The Measurement of Fixed Charge Density in the Intervertebral Disc," *Biochim. Biophys. Acta*, **586**, pp. 166–178.
- [24] Masuoka, K., Michalek, A. J., MacLean, J. J., Stokes, I. A. F., and Iatridis, J. C., 2007, "Different Effects of Static Versus Cyclic Compressive Loading on

- Rat Intervertebral Disc Height and Water Loss In Vitro,” *Spine*, **32**(18), pp. 1974–1979.
- [25] Gantenbein, B., Grunhagen, T., Lee, C. R., van Donkelaar, C. C., Alini, M., and Ito, K., 2006, “An In Vitro Organ Culturing System for Intervertebral Disc Explants With Vertebral Endplates: A Feasibility Study With Ovine Caudal Discs,” *Spine*, **31**(23), pp. 2665–2673.
- [26] van der Veen, A. J., van Dieen, J. H., Nadort, A., Stam, B., and Smit, T. H., 2007, “Intervertebral Disc Recovery After Dynamic or Static Loading In Vitro: Is There a Role for the Endplate?,” *J. Biomech.*, **40**(10), pp. 2230–2235.
- [27] MacLean, J. J., Owen, J. P., and Iatridis, J. C., 2007, “Role of Endplates in Contributing to Compression Behaviors of Motion Segments and Intervertebral Discs,” *J. Biomech.*, **40**(1), pp. 55–63.
- [28] Lee, C. R., Iatridis, J. C., Poveda, L., and Alini, M., 2006, “In Vitro Organ Culture of the Bovine Intervertebral Disc: Effects of Vertebral Endplate and Potential for Mechanobiology Studies,” *Spine*, **31**(5), pp. 515–522.